Journal of Physics: Condensed Matter

PAPER

2D $CrCl_2(pyrazine)_2$ monolayer: high-temperature ferromagnetism and half-metallicity

To cite this article: Huanhuan Xie *et al* 2020 *J. Phys.: Condens. Matter* **32** 135801

IOP Publishing Journal of Physics: Condensed Matter
J. Phys.: Condens. Matter **32** (2020) 135801 (5pp) https://doi.org/10.1088/1361-648X/ab5ca4

2D $CrCl_2(pyrazine)_2$ monolayer: high-temperature ferromagnetism and half-metallicity

Huanhuan Xie[1], Yu Qie[1], Imran Muhammad[1] and Qiang Sun[1,2,3]

[1] Department of Materials Science and Engineering, College of Engineering, Peking University, Beijing 100871, People's Republic of China
[2] Center for Applied Physics and Technology, Peking University, Beijing 100871, People's Republic of China

E-mail: sunqiang@pku.edu.cn

Received 9 October 2019, revised 15 November 2019
Accepted for publication 28 November 2019
Published 30 December 2019

Abstract

The ferromagnetism in Cr-based monolayers is of current interest (2019 *Nat. Nanotechnol.* **14** 408), however, the Curie temperature is low. How can we enhance the thermal stability of ferromagnetism? Motivated by the recent synthesis of the layered conductive magnet $CrCl_2(pyrazine)_2$ (2018 *Nat. Chem.* **10** 1056), we perform first-principles calculations and Monte Carlo simulations to demonstrate that the exfoliated 2D $CrCl_2(pyrazine)_2$ monolayer is stable dynamically and thermally, and it is a ferromagnetic half-metal with a sizeable band gap of 2.8 eV in the semiconducting channel, and the strong in-plane Cr–Cr interaction results in a large magnetic anisotropy energy. Moreover, the sheet exhibits a high Curie temperature of 350 K due to the enhanced magnetic exchange interaction resulting from the aromatic property of pyrazine. All of these intriguing features endow 2D $CrCl_2(pyrazine)_2$ sheet with good potentials for applications in nanoscale spintronics devices.

Keywords: ferromagnetism, 2D materials, half-metallicity, first principles calculations

(Some figures may appear in colour only in the online journal)

1. Introduction

Spintronics, also known as magnetoelectronics, has attracted widespread attention in science and industry [1–3]. Instead of using the charge of electrons, the spin degree freedom of electrons is used for information transfer and storage. For practical spintronic devices applications at room temperature, it is highly desirable to search for ferromagnetic materials with large spin polarization ratio, high Curie temperature (T_C), and large magnetic anisotropy energy (MAE) [4–8]. Moreover, for spintronic application at the nanoscale, it is crucial to develop low-dimensional ferromagnetic materials that possess the above properties [9–14] as shown by previous studies [15–19].Among them, 2D ferromagnetic sheets have been extensively studied for spin Nano devices due to the enhanced MAE resulting from the reduced dimensionality [20–22].

Recently a layered conductive magnet $CrCl_2(pyrazine)_2$ has been synthesized by reaction of $CrCl_2$ with pyrazine (pyz) [23] where Cr atoms distribute regularly and separately. Besides Cr, this synthesis technique is also applicable for other transition metal atoms, thus offering a pathway of using exfoliation to get magnetic 2D monolayers that can go beyond the Mermin–Wagner limit on stable long-range ferromagnetic order in monolayers [24], as demonstrated by previous theoretical prediction of 2D ferromagnetic monolayers CrX_3 (X = Cl, Br, I) [25] which have been confirmed by experiments [26, 27].

In this work, by performing first-principles calculations method and Monte Carlo (MC) simulations, we thoroughly investigate the electronic structure and magnetic properties of 2D $CrCl_2(pyz)_2$ sheet by focusing on the magnetic coupling

[3] Author to whom any correspondence should be addressed.

and magnetic behaviors. Our results show that the $CrCl_2(pyz)_2$ sheet is a stable half-metallic ferromagnetic material with 100% spin polarization at Fermi level, and exhibits a large MAE and a high T_C, which make it an ideal candidate material for spin-filtering.

2. Computational methods

Calculations are based on spin-polarized density functional theory (DFT) using the generalized gradient approximation (GGA) presented by Perdew–Burke–Ernzerhof (PBE) [28]. The projected augmented wave (PAW) method with a plane-wave basis set is used as implemented in the Vienna *ab initio* simulation package (VASP) [29, 30], and the cutoff kinetic energy is set to be 600 eV. We use the GGA+U method [31] with $U_{eff} = 4$ eV for the 3d orbital of Cr atoms that has been tested and compared with experiments [32, 33]. We use periodic boundary condition with a large vacuum slab of 20 Å along the *c*-direction to prevent the influence of the adjacent-layer interactions. Based on the convergence test, $9 \times 9 \times 1$ Monkhorst–Pack [34] *k*-point mesh is adopted to represent the reciprocal space of the unit cell. The structures are fully relaxed without any symmetric constraints, and the energy and force convergence criteria are set to be 10^{-6} eV and 0.01 eV $Å^{-1}$, respectively.

To check the dynamic stability, perturbation theory is used to calculate the lattice vibrational properties by optimizing the structures with a higher convergence criterion of 10^{-8} eV for total energy and 10^{-6} eV $Å^{-1}$ for force. Based on the dynamical matrix calculated by VASP, we use Phonopy code to calculate force constants and obtain the phonon band dispersions by solving the dynamical equations [35].

To ensure accurate electronic properties, we use HSE06 hybrid functional with 25% of the GGA exchange being replaced by exact Hartree–Fock exchange, and the exchange interaction being screened with a range separation parameter of 0.2 $Å^{-1}$, which can provide more accurate results of the band structure as widely accepted.

3. Results and discussion

Monolayer $CrCl_2(pyz)_2$ exhibits a symmetry of tetragonal P4/NBM space group with a unit cell of $a = b = 9.868$ Å, $\alpha = \beta = \gamma = 90°$, Cr–Cr distances of 6.977 Å and Cr–N bond lengths of 2.059 Å, as shown in figure 1, where the pyrazine rings are raked about the N–N axes with a uniform orientation at an angle of 36.5° to the planes of the Cr atoms, that is in agreement with the results reported by previous experimental and theoretical works [23].

The most possible way to obtain the 2D monolayer is to exfoliate it from layered structure. The calculated exfoliation energy is 12 meV $Å^{-2}$, which is smaller than the value of 21 meV $Å^{-2}$ for graphene [36], suggesting that 2D monolayer $CrCl_2(pyz)_2$ can be cleaved easily from the layered bulk phase.

To verify the dynamic stability, we calculate the phonon spectra which is shown in figure 1(c). There are no imaginary frequencies occur in the whole Brillouin zone. We also carry out *ab initio* molecular dynamics simulation at 500 K with a supercell, which shows slight changes in structure after heating for 5 ps. The simulated results are plotted in figure 1(d), where the potential energy only slightly fluctuates around the equilibrium value during the simulation, suggesting the thermal stability of $CrCl_2(pyz)_2$ sheet at room temperature.

To identify the stable magnetic state, spin-polarized calculations for ferromagnetic (FM) and antiferromagnetic (AFM) state are performed as illustrated in figures 2(a) and (b). In FM state, the main spin polarization comes from Cr atoms that are antiferromagnetically coupled with the adjacent N atoms (Cr ~ 3 μ_B, N ~ −0.25 μ_B) while other C, H, and Cl atoms are barely spin-polarized. In AFM state, the magnetic moments of adjacent Cr atoms are coupled oppositely. The exchange energy E_{ex} ($=E_{AF} - E_{FM}$) per unit cell is +220 meV, indicating that it is energetically more favorable for Cr atoms to ferromagnetically couple with each other in $CrCl_2(pyz)_2$ sheet, resulting in a total magnetic moment of 4 μ_B in each unit cell. In order to study the effect of U_{eff} value on magnetism, we calculated the energy of the system with different values (0–6 eV). As plotted in figure 2(c), we can see that FM state is always stable than AFM state for all the U_{eff} values adopted in our calculations.

The band structure and density of state (DOS) of 2D $CrCl_2(pyz)_2$ calculated with HSE06 hybrid functional are shown in figure 2(d), where the spin-up channel exhibits semiconducting property with a band gap of 2.8 eV while the spin-down electrons show metallic behavior which is mainly contributed by the p bands of the pyrazine ligand. According to the definition of spin polarizability: $\delta = |\rho\uparrow - \rho\downarrow|/(\rho\uparrow + \rho\downarrow)$, here $\rho\uparrow$ and $\rho\downarrow$ represent the density of spin-up and spin-down at the Fermi level, respectively, the $CrCl_2(pyz)_2$ sheet is a half-metal with 100% spin polarization ratio in the Fermi level and the half-metallic gap is 0.5 eV. Due to the half-metallic nature of the system, the spin-up electrons and the spin-down electrons are asymmetrically distributed, thus leading to magnetism. In addition, the coupling of p-d orbitals provides effective interaction between the Cr atoms and the pyrazine ligand, which results in a large exchange energy.

In order to analyze the magnetic properties of this system, we calculate the partial DOS of the d electrons of Cr atoms. As we know that in a stretched octahedral environment, the d orbitals are split into non-degenerate orbitals (d_{z2}, d_{xy}, d_{x2_y2}) and a doubly degenerate orbital (d_{xz} and d_{yz}). From the calculation results, we find that three spin-up d_{xz}, d_{yz}, and d_{x2-y2} orbitals of are occupied while all other orbitals are empty, thus giving rise to a magnetic moment of 3 μ_B per Cr atom.

Besides the magnetic moment, MAE is another important parameter for magnetic materials that is directly related to the information storage density. In current devices, one bit of information is stored in a few hundred single-domain particles or grains, which can be reduced when using materials with large MAE [16, 37]. Because reducing the dimensions and symmetry would result in a large MAE, we then can expect a large MAE in $CrCl_2(pyz)_2$ sheet, which is defined as $MAE = E_{\parallel} - E_{\perp}$, where $E_{\parallel}$ and $E_{\perp}$are energies when the magnetic axis is parallel or perpendicular to the 2D framework, respectively. The calculated MAE is 398 μeV per Cr

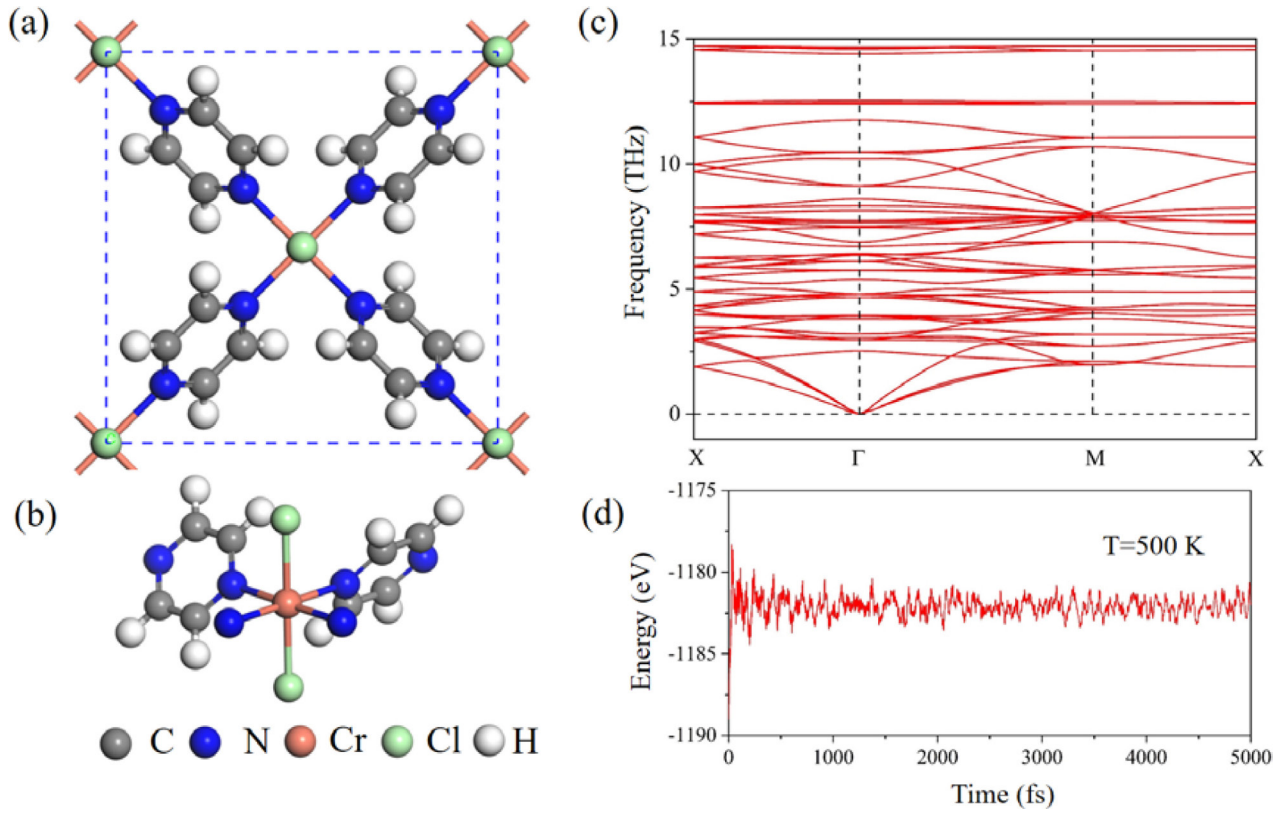

Figure 1. (a) Top view of the $CrCl_2(pyz)_2$ structure, (b) a fragment of the unit cell showing the rotation of the pyrazine rings. (c) Phonon spectra and (d) energy fluctuation during AIMD simulation at 500 K.

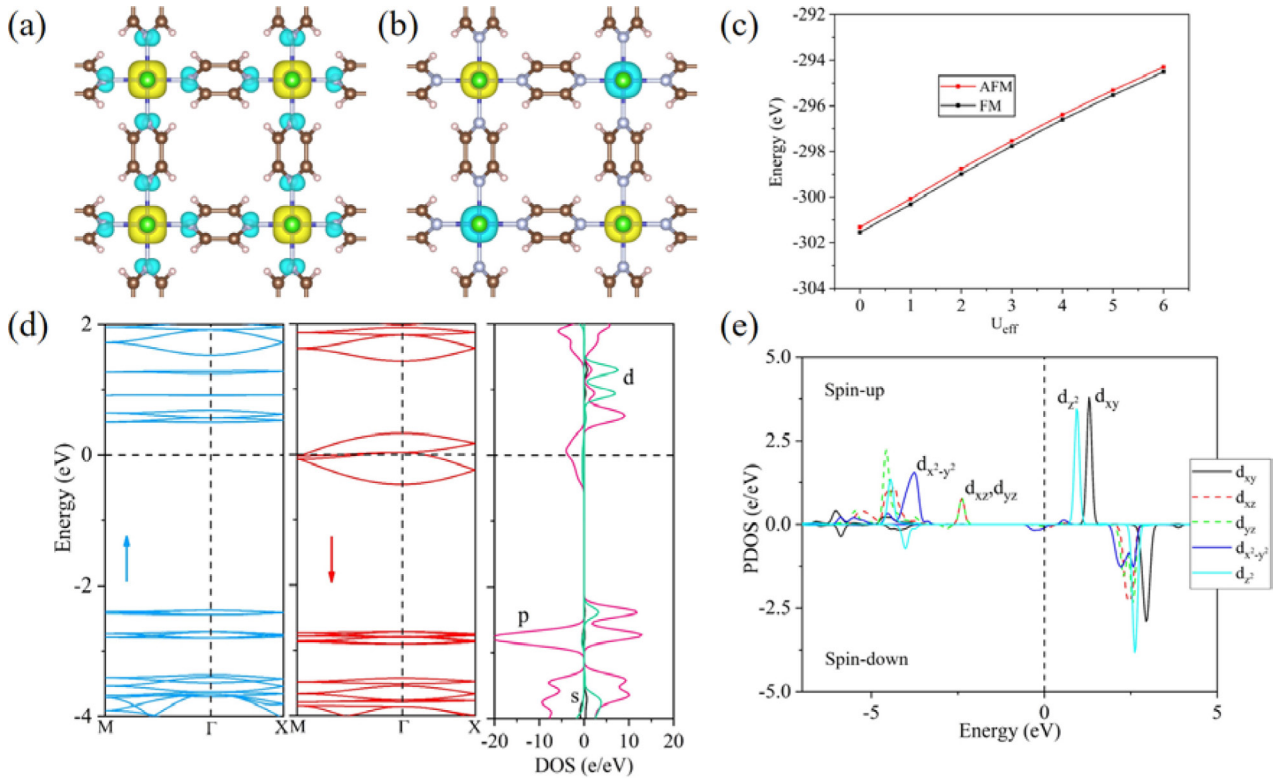

Figure 2. Spin density for (a) FM and (b) AFM 2D $CrCl_2(pyz)_2$ at an isosurface value of 0.012 e $Å^{-3}$. (c) Energy changes of FM and AFM states along with U_{eff}. (d) Band structure and (e) partial DOS of the ***d*** band of the Cr atom.

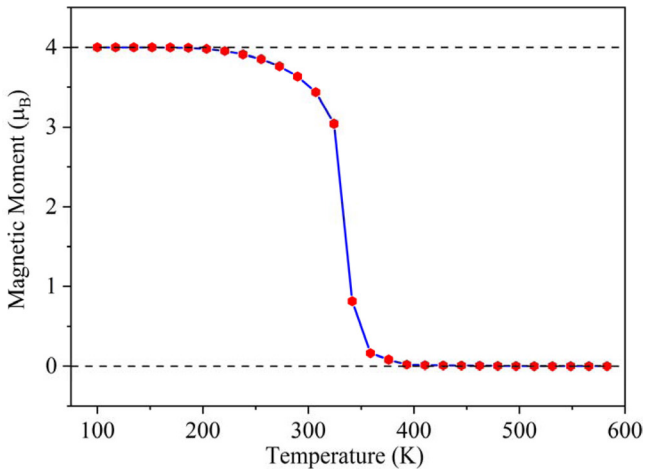

Figure 3. Total magnetic moment for each unit cell of $CrCl_2(pyz)_2$ sheet regarding to the temperature.

atom, which are about two orders larger than those of cubic Fe (1.4 μeV per atom), and Ni (2.7 μeV per atom) [38], such large MAE is rarely found in other low-dimensional materials [39–41], indicating the promising applications of $CrCl_2(pyz)_2$ sheet for magnetic memory devices.

For practical spintronic applications, the FM state needs to be stable over a wide temperature range. To this end, we next study how magnetism changes with temperature by using Ising model, in which the Hamiltonian can be written as $H = -\sum_{i,j} J m_i \cdot m_j$, where J is the exchange parameter and m_i and m_j are the sites i and site j magnetic moments. Here, we treat each chemical formula $CrCl_2(pyz)_2$ as one unit carrying magnetic moments with the possible values of $+2, 0, -2$ μ_B. J can be obtained by calculating the exchange energy E_{ex} defined as: $E_{ex} = E_{AFM} - E_{FM} = 4Jm^2 - (-4)Jm^2$, where m is magnetic moment, and the factor 4 presents four magnetic interactions in the unit cell. Therefore, we calculate the exchange parameter J, which is found to be 4.23 meV. Based on these results, we can estimate the Currie temperature by using mean-field theory (MFT), in which the partition function is in the following form

$$Z = \sum_{m=2,0-2} e^{-\beta\gamma Jm\langle m\rangle}.$$

Here $\gamma = 4$ is the coordinating number. Then the average magnetic moment in $CrCl_2(pyz)_2$ sheet can be calculated as

$$\langle m\rangle = \frac{1}{\beta}\frac{\partial}{\partial B}\ln Z.$$

Let $P = 2\beta\gamma J$, the equation above can be rewritten as

$$\langle m\rangle = \frac{2e^{P\langle m\rangle} - 2e^{-P\langle m\rangle}}{e^{P\langle m\rangle} + e^{-P\langle m\rangle} + 1}$$

the Currie temperature T_C for phase transition from ferromagnetic to paramagnetic states is estimated as ~479 K. To more accurately calculate T_C, we next perform MC simulations by using a (80×80) supercell and 5×10^5 loops. The spin states of each site of the system updated according to the spins of nearby atoms in each loop. Hence, totally 3.2×10^9 trials are carried out in the simulations. The MC simulation results are shown in figure 3. We have also checked a larger supercell and longer loops, while the results are almost unchanged. We can see that the paramagnetic state appears at the temperature of ~350 K for 2D $CrCl_2(pyz)_2$, indicating the T_C value is above room temperature. Especially, it is interesting to note that the Tc of $CrCl_2(pyz)_2$ sheet is much higher than that of $CrCl_3$ sheet, the underlying reason is following: different from $CrCl_3$ sheet, the magnetic coupling between Cr ions in $CrCl_2(pyz)_2$ sheet is mediated by pyrazine that is aromatic with delocalized electrons. In fact, ferromagnetic spin coupling mediated by π-conjugated ligand was confirmed in high-spin molecules in 1995 [42], and this kind mechanism has also been confirmed in K_3Fe_2[PcFe–O_8] MOF monolayer recently [43], where magnetization experiments and Fe Mössbauer spectroscopy demonstrate the presence of long-range magnetic correlations in K_3Fe_2[PcFe–O_8] arising from the magnetic coupling between iron centers via delocalized π electrons.

4. Conclusions

In summary, motivated by the recent experimental progress, we systematically investigate the electronic structure and magnetism of 2D $CrCl_2(pyz)_2$ monolayer. The results of the calculation lead to the following conclusions: (1) The $CrCl_2(pyz)_2$ monolayer is a half-metallic ferromagnet with 100% spin polarization and sizeable band gap of 2.8 eV; (2) Cr ions are ferromagnetically coupled with a total magnetic moment of 4 μ_B in one unit cell; (3) the easy axis of magnetization is along the normal direction of the sheet with a large MAE; (4) the ferromagnetism displayed in $CrCl_2(pyz)_2$ sheet shows high thermal stability with a Currie temperature of 350 K, which is much higher than that of $CrCl_3$ sheet. These intriguing features make $CrCl_2(pyz)_2$ sheet very promising for applications. We hope our theoretical research will promote further experimental effort on this subject.

Acknowledgments

This work is partially supported by grants from the National Natural Science Foundation of China (21573008 and 21773003), and from the National Key Research and Development Program of China (2017YFA0204902). The calculations are supported by the High-performance Computing Platform of Peking University.

ORCID iDs

Huanhuan Xie https://orcid.org/0000-0002-3292-9039
Imran Muhammad https://orcid.org/0000-0002-0193-0926

References

[1] Han W, Kawakami R K, Gmitra M and Fabian J 2014 Graphene spintronics *Nat. Nanotechnol.* **9** 794
[2] Tian Y, Shen S, Cong J, Yan L, Wang S and Sun Y 2016 Observation of resonant quantum magnetoelectric effect in

a multiferroic metal–organic framework *J. Am. Chem. Soc.* **138** 782–5
[3] Bodnar S Y, Smejkal L, Turek I, Jungwirth T, Gomonay O, Sinova J, Sapozhnik A A, Elmers H J, Klaui M and Jourdan M 2018 Writing and reading antiferromagnetic Mn_2Au by Neel spin-orbit torques and large anisotropic magnetoresistance *Nat. Commun.* **9** 348
[4] Deng Y *et al* 2018 Gate-tunable room-temperature ferromagnetism in two-dimensional Fe_3GeTe_2 *Nature* **563** 94–9
[5] Lehnert A, Dennler S, Błoński P, Rusponi S, Etzkorn M, Moulas G, Bencok P, Gambardella P, Brune H and Hafner J 2010 Magnetic anisotropy of Fe and Co ultrathin films deposited on Rh(1 1 1) and Pt(1 1 1) substrates: an experimental and first-principles investigation *Phys. Rev.* B **82** 094409
[6] Zhou X, Zhang R W, Zhang Z, Ma D S, Feng W, Mokrousov Y and Yao Y 2019 Fully spin-polarized nodal loop semimetals in alkaline metal monochalcogenide monolayers *J. Phys. Chem. Lett.* **10** 3101–8
[7] Zheng S, Huang C, Yu T, Xu M, Zhang S, Xu H, Liu Y, Kan E, Wang Y and Yang G 2019 High-temperature ferromagnetism in an Fe_3P monolayer with a large magnetic anisotropy *J. Phys. Chem. Lett.* **10** 2733–8
[8] Torelli D and Olsen T 2018 Calculating critical temperatures for ferromagnetic order in two-dimensional materials *2D Mater.* **6** 015028
[9] Zhou J and Sun Q 2011 Magnetism of phthalocyanine-based organometallic single porous sheet *J. Am. Chem. Soc.* **133** 15113–9
[10] Kan M, Zhou J, Sun Q, Kawazoe Y and Jena P 2013 The intrinsic ferromagnetism in a MnO_2 monolayer *J. Phys. Chem. Lett.* **4** 3382–6
[11] Song T *et al* 2018 Giant tunneling magnetoresistance in spin-filter van der Waals heterostructures *Science* **360** 1214–8
[12] Wang A, Zhang X, Feng Y and Zhao M 2017 Chern insulator and chern half-metal states in the two-dimensional spin-gapless semiconductor $Mn_2C_6S_{12}$ *J. Phys. Chem. Lett.* **8** 3770–5
[13] Huang C, Feng J, Wu F, Ahmed D, Huang B, Xiang H, Deng K and Kan E 2018 Toward intrinsic room-temperature ferromagnetism in two-dimensional semiconductors *J. Am. Chem. Soc.* **140** 11519–25
[14] Zhang M, Wang X, Sun H, Yu J, Wang N, Long Y and Huang C 2018 Preparation of room-temperature ferromagnetic semiconductor based on graphdiyne-transition metal hybrid *2D Mater.* **5** 035039
[15] Kan E, Hu W, Xiao C, Lu R, Deng K, Yang J and Su H 2012 Half-metallicity in organic single porous sheets *J. Am. Chem. Soc.* **134** 5718–21
[16] Li X, Wu X and Yang J 2014 Room-temperature half-metallicity in La(Mn,Zn)AsO alloy via element substitutions *J. Am. Chem. Soc.* **136** 5664–9
[17] Liu H, Sun J T, Liu M and Meng S 2018 Screening magnetic two-dimensional atomic crystals with nontrivial electronic topology *J. Phys. Chem. Lett.* **9** 6709–15
[18] Hashmi A, Farooq M U and Hong J 2016 Long-range magnetic ordering and switching of magnetic state by electric field in porous phosphorene *J. Phys. Chem. Lett.* **7** 647–52
[19] Huang C, Du Y, Wu H, Xiang H, Deng K and Kan E 2018 Prediction of intrinsic ferromagnetic ferroelectricity in a transition-metal halide monolayer *Phys. Rev. Lett.* **120** 147601
[20] Huang B *et al* 2017 Layer-dependent ferromagnetism in a van der Waals crystal down to the monolayer limit *Nature* **546** 270–3
[21] Gong C *et al* 2017 Discovery of intrinsic ferromagnetism in two-dimensional van der Waals crystals *Nature* **546** 265–9
[22] Jang S W, Jeong M Y, Yoon H, Ryee S and Han M J 2019 Microscopic understanding of magnetic interactions in bilayer CrI_3 *Phys. Rev. Mater.* **3** 031001
[23] Pedersen K S *et al* 2018 Formation of the layered conductive magnet $CrCl_2(pyrazine)_2$ through redox-active coordination chemistry *Nat. Chem.* **10** 1056–61
[24] Mermin N D and Wagner H 1966 Absence of ferromagnetism or antiferromagnetism in one- or two-dimensional isotropic heisenberg models *Phys. Rev. Lett.* **17** 1133–6
[25] Liu J, Sun Q, Kawazoe Y and Jena P 2016 Exfoliating biocompatible ferromagnetic Cr-trihalide monolayers *Phys. Chem. Chem. Phys.* **18** 8777–84
[26] Kim H H *et al* 2019 Evolution of interlayer and intralayer magnetism in three atomically thin chromium trihalides *Proc. Natl Acad. Sci.* **116** 11131–6
[27] Gibertini M, Koperski M, Morpurgo A F and Novoselov K S 2019 Magnetic 2D materials and heterostructures *Nat. Nanotechnol.* **14** 408–19
[28] Perdew J P, Burke K and Ernzerhof M 1996 Generalized gradient approximation made simple *Phys. Rev. Lett.* **77** 3865
[29] Kresse G and Furthmüller J 1996 Efficient iterative schemes for *ab initio* total-energy calculations using a plane-wave basis set *Phys. Rev.* B **54** 11169
[30] Kresse G and Joubert D 1999 From ultrasoft pseudopotentials to the projector augmented-wave method *Phys. Rev.* B **59** 1758
[31] Dudarev S, Botton G, Savrasov S, Humphreys C and Sutton A 1998 Electron-energy-loss spectra and the structural stability of nickel oxide: an LSDA+U study *Phys. Rev.* B **57** 1505
[32] Bernien M, Miguel J, Weis C, Ali M E, Kurde J, Krumme B, Panchmatia P M, Sanyal B, Piantek M and Srivastava P 2009 Tailoring the nature of magnetic coupling of Fe-porphyrin molecules to ferromagnetic substrates *Phys. Rev. Lett.* **102** 047202
[33] Sato K *et al* 2010 First-principles theory of dilute magnetic semiconductors *Rev. Mod. Phys.* **82** 1633–90
[34] Monkhorst H J and Pack J D 1976 Special points for Brillouin-zone integrations *Phys. Rev.* B **13** 5188
[35] Togo A and Tanaka I 2015 First principles phonon calculations in materials science *Scr. Mater.* **108** 1–5
[36] Jung J H, Park C-H and Ihm J 2018 A rigorous method of calculating exfoliation energies from first principles *Nano Lett.* **18** 2759–65
[37] Sun Y, Zhuo Z, Wu X and Yang J 2017 Room-temperature ferromagnetism in two-dimensional Fe_2Si nanosheet with enhanced spin-polarization ratio *Nano Lett.* **17** 2771–7
[38] Daalderop G H O, Kelly P J and Schuurmans M F H 1990 First-principles calculation of the magnetocrystalline anisotropy energy of iron, cobalt, and nickel *Phys. Rev.* B **41** 11919–37
[39] Choudhuri I and Pathak B 2017 Ferromagnetism and half-metallicity in atomically thin holey nitrogenated graphene based systems *ChemPhysChem* **18** 2336–46
[40] Kuklin A V, Shostak S A and Kuzubov A A 2018 Two-dimensional lattices of VN: emergence of ferromagnetism and half-metallicity on nanoscale *J. Phys. Chem. Lett.* **9** 1422–8
[41] Feng W, Guo G-Y and Yao Y 2016 Tunable magneto-optical effects in hole-doped group-IIIA metal-monochalcogenide monolayers *2D Mater.* **4** 015017
[42] Rajca S and Rajca A 1995 Novel high-spin molecules:. pi.-conjugated polyradical polyanions. ferromagnetic spin coupling and electron localization *J. Am. Chem. Soc.* **117** 9172–9
[43] Yang C, Dong R, Wang M, Petkov P S, Zhang Z, Wang M, Han P, Ballabio M, Bräuninger S A and Liao Z 2019 A semiconducting layered metal-organic framework magnet *Nat. Commun.* **10** 3260